FRACTAL ESTIMATION IN A GIVEN FREQUENCY RANGE. APPLICATION TO SMECTITE IMAGES.

R. Harba, M. Cintract*, M. Zabat**, H. Van Damme***

* Laboratoire d'Electronique, Signaux, Images, Université d'Orléans
12 rue de Blois, BP 6744, 45067 Orléans Cedex 2, France.
Tel : (33) 02 38 41 72 29 ; fax : (33) 02 38 41 72 45 ; e-mail : harba@lesi.univ-orleans.fr
** Centre de Recherche sur la Matière Divisée, CNRS et Université d'Orléans
45067 Orléans Cedex 2, France.
Tel : (33) 02 38 25 53 79 ; e-mail : mokhtar@cnrs-orleans.fr

ABSTRACT

In this communication, an efficient fractal estimation is proposed in a given frequency range. It is based on the maximum likelihood Whittle approximation for the stationary increments of fractional Brownian motion. Its efficiency is first shown on synthetic data generated by the Cholesky method. Then it is applied to smectite deposits on films analyzed by atomic force microscope. It is shown that the fractal parameter measured in the low frequency region allows to separate 3 groups of smectite clay images, and enables to recover chemical properties of the material.

1 INTRODUCTION

Fractional Brownian motion (fBm) is a non-stationary stochastic process widely used to model 1/f behavior [1]. In the time or scale domains, such a process is statistically self-similar. More precisely, z-axis fluctuations are related to x-axis increments by $\mathrm{var}(\Delta z) \propto \Delta x^{2H}$. H such that 0<H<1 is the Hurst exponent. H close to 0 corresponds to rough signals or images, while they are smooth for H close to 1. In many cases, as for example smectite images [2] or bone texture radiographs [3], the fractal character is scale limited or identically, frequency limited. In such cases, it would be interesting to measure the fractal dimension in the region where data are self-similar. A method to properly measure H *i.e.* choosing a reliable estimator and being able to measure H at a scale or frequency range of interest is needed.

The object of this communication is an attempt to estimate the H parameter in a given frequency range. In the first part, main results of a recent study comparing the efficiency of fractal estimators will be presented. Then, a measurement in a frequency range of interest will be proposed. Finally, it will be applied to smectite images where a 1/f behavior is experimentally observed in the low frequency region. Results of H measurements will be compared to standard surface roughness attributes.

2 EFFICIENT FRACTAL ESTIMATION

The efficiency of H estimators can be assessed on reference synthesized fractal signals [4]. This last study has shown that among 5 synthesis methods currently used in signal processing, only the Cholesky decomposition of the covariance matrix of the process increments method [5] and the Weirstrass-Mandelbrot function [6] produce proper fBm signals. Then, a set of reference signals was generated on which 8 fractal estimators were tested [7]. The bias is the difference between the H value of synthesized true fBm signals and the mean H value for a given estimator. The variance is compared to the Cramer-Rao lower bound (CRLB) which can be calculated using results in [8]. The maximum likelihood method (ML) [5], the variance method (VAR) [9] and the Wavelet method (WAA) [10] give good results concerning the bias. But, only ML has a variance close to the CRLB even for a short data length. However, some practical limitations may be reported for this last method. Inverse and determinant of a $N \times N$ matrix have to be calculated. Even if the Levinson algorithm was used for this Toeplitz matrix [11], the computer burden is expensive and the size of the studied vector is limited (1024 samples for a memory size of 32MB). But, even more important when it is applied to experimental data having limited self-similar behavior, this method cannot measure the fractal dimension in a given scale range or in a frequency range while VAR and WAV can.

3 EFFICIENT FRACTAL ESTIMATOR IN A GIVEN FREQUENCY RANGE

This estimator should be a ML based one because of its efficiency but operating either in the scale or frequency domain. Thus, selecting an appropriate range would be possible. Before presenting an approximation due to Whittle in the frequency domain, main steps for the classical ML H estimates are to be recalled. It is based on the fBm model or on its increments, the fractional Gaussian noise (fGn) which is stationary. Since they are both zero mean Gaussian processes, their log likelihood function (LLF) with respect to H can be directly expressed (constant terms are neglected):

$$\mathrm{LLF(H)} = -\log\left|\mathrm{R}\right| - \mathrm{V}^{\mathrm{T}}\,\mathrm{R}^{-1}\,\mathrm{V}\ . \qquad (1)$$

V is the observed vector (either fBm of fGn) and R is the corresponding theoretical normalized covariance matrix depending on H. The ML H value correspond to the maximum of (1) in the interval]0,1[.

The Whittle approximation operates in the frequency domain in the case of a stationary process [12]. Thus, only fGn can be considered for our particular case. The Whittle approximated log likelihood function, LLFw, with respect to H is the following:

$$\mathrm{LLFw(H)} = \int_{-\infty}^{\infty}\left(-\log(\mathrm{T}) - \frac{\hat{\mathrm{E}}}{\mathrm{T}}\right)df\,. \qquad (2)$$

T is the theoretical power spectral density (PSD) of fGn and $\hat{\mathrm{E}}$ is the estimated PSD for a given vector increments. The former is computed by Fourier transform of the theoretical covariance function depending on H and the latter by the square modulus of the Fourier transform of data increments. The Whittle ML H value correspond to the maximum of (2) in the interval]0,1[.

The efficiency of the Whittle approximation can be compared to the classical ML estimates on reference signals. 100 vectors of 256 samples each were generated using the CHO method [5]. Results concerning the mean H value as well as the standard deviation (STD) for both estimators are presented in table 1 for 3 H values. The square root of the CRLB allows to evaluate their respective quality.

A bilateral Student t test shows that both estimators are unbiased and a right-sided unilateral F test shows that both estimators are equal to the CRLB. Tests are performed with a level of significance of 0.01. Thus, both methods are efficient. But, compared to the classical ML one, the Whittle approximation is less time consuming and can operate in a frequency range of interest as shows table 2. Here, estimation is performed on a reduced frequency range, first in the low frequency region (from 0 to fs/4 with fs the sampling period) and then for high frequencies (from fs/4 to fs/2).

	$\langle\hat{\mathrm{H}}\rangle$ Whittle	STD Whittle	$\langle\hat{\mathrm{H}}\rangle$ ML	STD ML	$\sqrt{\mathrm{CRLB}}$
H=0.2	0.208	0.032	0.201	0.031	0.030
H=0.5	0.497	0.040	0.498	0.041	0.039
H=0.8	0.796	0.043	0.798	0.042	0.039

Table 1 : mean H estimated value ($\langle\hat{\mathrm{H}}\rangle$) and standard deviation (STD) compared to the Cramer-Rao lower bound (CRLB) for both Whittle and ML estimators on 100 signals of 256 samples generated by the Cholesky method.

	0 to fs/4		fs/4 to fs/2	
	$\langle\hat{\mathrm{H}}\rangle$ Whittle	STD Whittle	$\langle\hat{\mathrm{H}}\rangle$ Whittle	STD Whittle
H=0.2	0.213	0.046	0.270	0.247
H=0.5	0.497	0.059	0.498	0.269
H=0.8	0.786	0.061	0.732	0.230

Table 2 : mean H estimated value ($\langle\hat{\mathrm{H}}\rangle$) and standard deviation (STD) for the Whittle estimator on 100 signals of 256 samples generated by the Cholesky method. It is first presented in the low frequency region (0 to fs/4) and then in the high frequency one (fs/4 to fs/2).

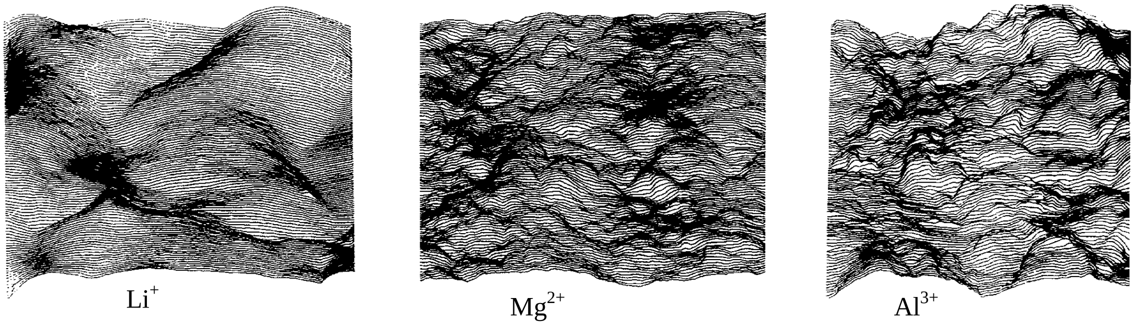

Figure 1 : Atomic microscope images of smectite clays deposits on films for respectively Li^{+}, Mg^{2+} and Al^{3+} in the suspension. The resolution of the images is of 16 microns.

In the low frequency region, the Whittle approximation gives good results. But, it is severely affected by statistical fluctuations in the high frequency one. Indeed, due to the 1/f structure of fractal signals, a few of the total energy of the signal rely in the high frequency region and could explain these poor results. In this case, averaging in the frequency domain would be necessary before estimating the H parameter.

4 APPLICATION TO SMECTITE IMAGES

A lot of surfaces generated by irreversible growth (deposition, fracture) exhibit a fractal character [13][14]. It is the case of smectite clay surfaces. The final stage of the deposition process is the concentrated regime when the clay becomes a dry rock. Depending on the cations present in the suspensions, two extreme situations may be considered: thin and deformable aggregates for low charge and strongly hydrated cations (entangled clays) and thick and rigid aggregates for strongly polarizing and weakly hydrated cations (stacked clays). The nature of the aggregate is of a great importance because a lot of the material properties (mechanical, optical, porosity, ...) are strongly related to it. To recover the nature of the aggregate, an image analysis can be performed. At small scales or conversely at high frequencies, the roughness of the aggregate is revealed which is not discriminative. At large scale or conversely at low frequencies, entangled clays should produce smooth surfaces while they should be rough for stacked clays. In Figure 1, atomic force microscope images of smectite clays are presented for respectively Li^{+} (entangled clays), Mg^{2+} and Al^{3+} (stacked clays) in the suspension. The scale of 16 microns can reveal the evolution both at small and high scale.

As expected, images are globally smooth for entangled clays and rough for stacked clays. Within this last group, no low trends are visible on the image of Mg^{2+} while a low trend can be seen on Al^{3+} image. Thus, we can define 3 groups. Group I: entangled clays having smooth surfaces with low trends (Li^{+}); Group II: stacked clays having rough surfaces with no low trend (Mg^{2+}) ; Group III: stacked clays having rough surfaces with low trends (Al^{3+}). A frequency study of these images is shown in figure 2 where the Power Spectral Density (PSD) of the increments of image lines are represented in a log-log scale for the same cations as figure 1 and in the low frequency region. If present, the fractal character is equivalent to straight lines of slope 1-2H (0<H<1).

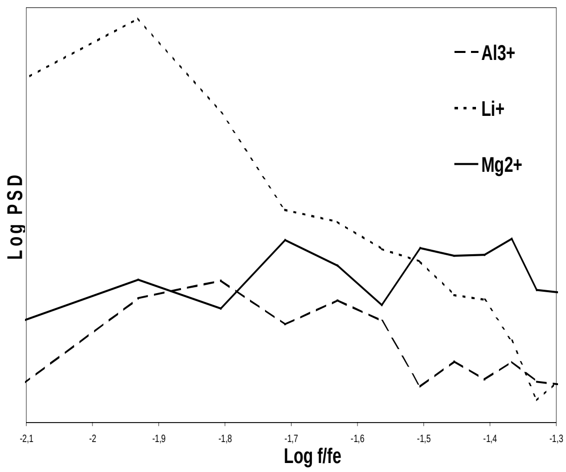

Figure 2 : PSD in the low frequency region of the increments of image lines of figure 1 in a log-log plot.

As seen, curves are almost linear in the low frequency region and slopes are quite different in the 3 cases. Thus, the H parameter can be measured in the low frequency region using the Whittle approximation as previously explained. Classical roughness attributes can also been computed: the peak-to-valley (PV) distance (altitude distance between highest and lowest point) and the root mean square (RMS) distance are also of interest (standard deviation of the altitudes). The next table shows the mean H parameter estimated in the low frequency using the Whittle approximation, the mean PV and mean RMS distances on 4 images for each group.

	H Whittle	PV (microns)	RMS (microns)
Group I	0.705 ±0.076	1.72 ± 0.334	0.570 ± 0.787
Group II	0.207 ± 0.040	1.19 ± 0.403	0.247 ± 0.437
Group III	0.410 ± 0.132	1.60 ± 0.585	0.532 ± 0.207

Table 3 : average H parameter, PV and RMS distances on 4 images of Group I, II and III.

Due to the few samples that were available (only 4 in each group), statistical tests are not significant. However, it can be seen that the PV distance is identical in Groups I and III (both having low trends) but is different for Group II (no low trend). The RMS distance shows the same behavior. Only the low frequency H parameter has different values for the 3 groups. It is then possible to discriminate between these 3 groups using the low frequency H parameter while classical roughness attributes cannot. Thus, chemical properties of the material can be recovered by a fractal image analysis procedure.

5 CONCLUSION

In this communication, we have proposed a fractal estimation in a given frequency range based on the maximum likelihood Whittle approximation. This method is efficient on synthesized fBm signals. But, at the opposite of the classical ML one, it is able to measure the fractal dimension in a frequency area of interest.

This method was applied to smectite clay atomic force microscope images to estimate the low frequency H parameter. This characteristic is related to the nature of the aggregate leading to smooth or rough surfaces, low trends or no low trend images. Results show that H enables to separate 3 groups of images while classical roughness attributes cannot. Thus, it is possible to recover chemical properties of the material conditioning other characteristics (mechanical, optical, porosity, ...) by a fractal image analysis tool.

REFERENCES

[1] B. B. Mandelbrot, J. W. Van Ness, "Fractional Brownian Motion, Fractional Noises and Applications", *SIAM*, Vol. 10, N° 4, pp. 422-438, 1968.

[2] M. Zabat, M. Vayer-Besançon, R. Harba, S. Bonnamy, H. Van Damme, *"Surface Topography and Mechanical Properties of Smectite Films"*, Progr. Colloïd Polym. Sci., Vol. 105, pp. 96-102, 1997.

[3] R. Harba, G. Jacquet, R. Jennane, T. Loussot, C. L. Benhamou, E. Lespessailles, D. Tourlière, *"Determination of Fractal Scales on Trabecular Bone X-Ray Images"*, Fractals, Vol. 2, N° 3, pp. 451-456, 1994.

[4] R. Jennane, R. Harba, G. Jacquet, *"Estimation de la Qualité des Méthodes de Synthèse du Mouvement Brownien Fractionnaire"*, Traitement du Signal, Vol. 3, N° 4, pp. 289-302, 1997.

[5] T. Lundahl, W. J. Ohley, S. M. Kay, R. Siffert, *"Fractional Brownian Motion: A Maximum Likelihood Estimator and Its Application to Image Texture"*, IEEE Transactions on Medical Imaging, Vol. MI-5, N° 3, pp. 152-161, September 1986.

[6] M. V. Berry, Z. V. Lewis., *"On the Weierstrass-Mandelbrot Fractal Function"*, Procceedings of the Royal Society of London, Vol. A370, pp. 459-484, 1980.

[7] R. Jennane, R. Harba, G. Jacquet, *"Quality of Synthesis and Analysis Methods for Fractional Brownian Motion"*, IEEE DSP Workshop, pp. 307-310, 1996.

[8] S. M. Kay, *"Fundamentals of Statistical Signal Processing,"*, Englewood Cliffs, New Jersey : Prentice Hall International Editions, 1992.

[9] A. P. Pentland, *"Fractal-Based Description of Natural Scenes"*, IEEE Transactions on Pattern Analysis and Machine Intelligence, N° 6, pp. 661-674, November 1984.

[10] P. Flandrin, *"Wavelet Analysis and Synthesis of Fractional Brownian Motions"*, IEEE Transactions on Information Theory, Vol. 38, N° 2, pp. 910-917, March 1992.

[11] S. M. Kay, *"Modern Spectral Estimation: Theory and Application"*, Englewood Cliffs : Prentice Hall International Editions, 1988.

[12] R. Azencottt, D. Dacuna-Castelle, *"Séries d'Observations Irrégulières"*, Masson Editions, Paris, 1984.

[13] A. L. Barabasi, H. E. Stanley, *"Fractal Concepts in Surfaces Growth"*, Cambridge University Press, 1995.

[14] B. B. Mandelbrot, D. E. Passoja, A. J. Paullay, *"Fractal Character of Fracture Surfaces of Metal"*, Nature, Vol. 308, pp. 721-722, 1984.